

Binding energy and nature of the orbitals in fluorinated graphene: a density functional theory study

F Marsusi^{1*}, N D Drummond²

¹Department of Energy Engineering and Physics, Amirkabir University of Technology, PO Box 15875-4413, Tehran, Iran

E-mail: marsusi@aut.ac.ir

²Department of Physics, Lancaster University, Lancaster LA1 4YB, United Kingdom

E-mail: n.drummond@lancaster.ac.uk

August 2017

Abstract. We present density functional theory calculations of the binding energies of one, two and three fluorine adatoms on the same side of monolayer graphene. We show that fluorine dimers on graphene in a spin-singlet state are stable against dissociation into isolated fluorine adatoms, suggesting that there is a tendency for fluorine adatoms on a single side of graphene to cluster. Our results suggest that fluorination develops by successive bonding of fluorine atoms to neighbouring carbon atoms on different sublattices, while the spins are arranged to reduce the total magnetisation of the ground state. We find that the finite-size error in the binding energy of a single fluorine atom or dimer on a periodic supercell of graphene scales inversely with the cube of the linear size of the simulation supercell. By using π -orbital axis analysis, the rehybridisation of the three σ -orbitals pointing directly along the bonds to the central fluorinated carbon is found to be $sp^{2.33}$. The rehybridisation of the carbon orbital in the C-F bond is found to be $sp^{4.66}$.

PACS numbers: 81.05.ue, 68.35.Np, 71.15.Mb

Keywords: Graphene, fluorination

Submitted to: *J. Phys.: Condens. Matter*

1. Introduction

The fabrication of logic circuits based on graphene requires the ability to open a gap in its electronic band structure. Functionalising graphene with adatoms and admolecules is therefore of significant interest for the development of graphene-based electronic applications [1, 2]. Adatoms can significantly perturb the electronic structure

of graphene, leading to the formation of mid-gap states and the extreme modification of the opto-electronic and transport properties. However, to be practicable, graphene functionalised with adatoms or admolecules of interest should be stable, even at high temperatures. Hydrogen is one possible candidate for the band-gap engineering of graphene [3]. However, hydrogenated graphene suffers from instability at moderate temperatures, restricting its applicability [3]. On the other hand, fluorine is a particularly attractive adatom, and it has been confirmed that the thermal stability of fluorinated graphene is even higher than that of pristine graphene [4]. Previously, it has been shown that a single fluorine adatom prefers to sit directly above a carbon atom [5, 6, 7]. According to the literature, the binding energy ΔE_B of a fluorine adatom on graphene is significantly larger than that of many other adatoms [6, 8]. While the binding energy of a single adatom is important as a measure of the stability of fluorinated graphene, many of its physical properties depend on the geometry and arrangement of multiple fluorine adatoms. In this work we perform first-principles density functional theory (DFT) calculations to investigate the binding energy and atomic and electronic structure of a group of two or three fluorine adatoms on graphene. This information will allow the subsequent investigation of the thermodynamics of the fluorination process. We focus on the case in which the fluorine adatoms are on the same side of the graphene layer.

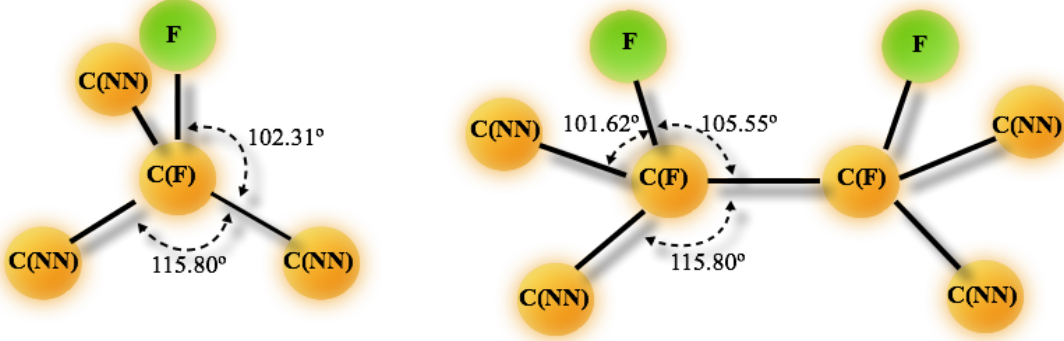
We have calculated the binding energies of single adatoms and pairs of adatoms (dimers) on the same side of $m \times m$ supercells of monolayer graphene subject to periodic boundary conditions, where $m = 2, 3, 4, 5, 6$ and 7 . Population analysis confirms that the adatoms set up an electric dipole moment along the C–F bond, suggesting that finite-size effects in the binding energy due to the repulsive interaction between the images of the dipole moments go as $-L^{-3}$, where L is the linear size of the supercell. We have used our results to compute the energy required to separate a fluorine dimer on one side of graphene into two isolated single adatoms in the dilute limit, and hence have shown that single-side dimer-fluorinated graphene is expected to be stable.

By calculating the binding energies of single and multiple fluorine adatoms, we show how fluorination is established geometrically on a single side of graphene and how the electron spins are arranged in the ground state of fluorinated graphene to increase the binding energy and to reduce the magnetisation M of the structure. Our findings are in agreement with the experimental observation that the measured number of paramagnetic centres is three orders of magnitude less than the number of fluorine adatoms in fluorinated graphene samples [9].

2. Computational details

The optimised geometries and binding energies of fluorine adatoms on monolayer graphene were obtained within the plane-wave–pseudopotential DFT framework implemented in the ABINIT code [10]. Both the local density approximation (LDA) and the Perdew–Burke–Ernzerhof (PBE) [11] exchange–correlation functionals were used.

Figure 1. (a) Single fluorine adatom on graphene. (b) Two fluorine adatoms (dimer) on graphene.



The cutoff energy on the plane-wave basis set was 40 Ha, and all atomic positions and in-plane lattice vectors were relaxed until the atomic forces were less than 6 meV/Å. A vacuum region of about 19 Å along the z axis was imposed to guarantee a vanishing interaction between the periodically repeated images of the graphene layer. The binding energies of a single fluorine adatom and a pair of fluorine adatoms on graphene were calculated in supercells of different size, to allow extrapolation to the dilute limit. A $5 \times 5 \times 1$ Monkhorst-Pack \mathbf{k} -point mesh was used to sample the Brillouin zone [12] in the largest supercells, with a finer sampling for smaller supercells. Norm-conserving Troullier–Martins pseudopotentials were used to represent the atomic cores [13, 14]. All our calculations were performed with spin-polarised wave functions, unless otherwise stated.

3. Results and discussion

3.1. Optimised geometries and nature of the orbitals

The LDA- and PBE-optimised geometrical parameters of a single fluorine adatom and a pair of fluorine adatoms on different supercells of graphene are shown in tables 1, 2 and 3. The atomic structure models are illustrated in figure 1.

After full relaxation, a single fluorine adatom remains exactly on top of a carbon atom, as expected. However, the repulsive force between two fluorine adatoms on top of neighbouring carbon atoms makes them relocate from their initial positions, as shown in figure 1(b). The geometry around the fluorine adatom appears to be converged with respect to size in a 7×7 supercell. Let C(F) denote the carbon atom to which the fluorine adatom is bonded. In a single adatom on graphene, the C(F)–F bond length is predicted to be about 1.55 Å, which is larger than the typical C–F sp^3 bond length (about 1.37 Å), and is in good agreement with a previous PBE prediction [15]. Other geometric information, including the distance between C(F) and its nearest neighbours C(NN), is presented in tables 1, 2 and 3. As a consequence of the attractive interaction between the carbon and fluorine atoms, C(F) is pulled out of the plane by about 0.33 Å

Table 1. LDA-optimised geometry and binding energy of a single fluorine adatom on graphene for different supercells ($m \times m$). $z(\text{C}(\text{F}))$ and $z(\text{C}(\text{NN}))$ are the z -coordinates of the carbon atom C(F) bonded to the fluorine and its nearest neighbour C(NN), respectively. C(F)–F and C(F)–C(NN) denote the bond lengths of the fluorine adatom to the carbon atom that it sits above and the bond length from that carbon atom to one of its nearest neighbours, respectively. $\angle \text{C}(\text{NN}), \text{C}(\text{F}), \text{F}$ denotes the tetrahedral angle and $\angle \text{C}(\text{NN}), \text{C}(\text{F}), \text{C}(\text{NN})$ denotes the hexagonal internal angle.

	3×3 cell	6×6 cell	7×7 cell
$z(\text{C}(\text{F})) - z(\text{C}(\text{NN}))$	0.32 Å	0.32 Å	0.32 Å
C–F	1.53 Å	1.52 Å	1.54 Å
C(F)–C(NN)	1.47 Å	1.47 Å	1.47 Å
$\angle \text{C}(\text{NN}), \text{C}(\text{F}), \text{F}$	102.44°	102.40°	102.26°
$\angle \text{C}(\text{NN}), \text{C}(\text{F}), \text{C}(\text{NN})$	115.49°	115.52°	115.62°
ΔE_{B}	2.32 eV	2.36 eV	

Table 2. PBE-optimised geometry and binding energy of a single fluorine adatom on graphene for different supercells ($m \times m$). $z(\text{C}(\text{F}))$ and $z(\text{C}(\text{NN}))$ are the z -coordinates of the carbon atom C(F) bonded to the fluorine and its nearest neighbour C(NN), respectively. C(F)–F and C(F)–C(NN) denote the bond lengths of the fluorine adatom to the carbon atom that it sits above and the bond length from that carbon atom to one of its nearest neighbours, respectively. $\angle \text{C}(\text{NN}), \text{C}(\text{F}), \text{F}$ denotes the tetrahedral angle and $\angle \text{C}(\text{NN}), \text{C}(\text{F}), \text{C}(\text{NN})$ denotes the hexagonal internal angle. For comparison with a fluorine adatom, we also present the value of the binding energy ΔE_{B} of a single hydrogen adatom in a 3×3 cell, together with the corresponding value obtained in a previous work [7] using the PBE functional.

	3×3 cell	4×4 cell	6×6 cell	7×7 cell
$z(\text{C}(\text{F})) - z(\text{C}(\text{NN}))$	0.31 Å	0.32 Å	0.31 Å	0.30 Å
C–F	1.55 Å	1.55 Å	1.56 Å	1.58 Å
C(F)–C(NN)	1.48 Å	1.48 Å	1.48 Å	1.47 Å
$\angle \text{C}(\text{NN}), \text{C}(\text{F}), \text{F}$	102.46°	102.52°	102.31°	101.96°
$\angle \text{C}(\text{NN}), \text{C}(\text{F}), \text{C}(\text{NN})$	115.47°	114.44°	115.56°	115.82°
ΔE_{B}	1.87 eV	1.93 eV	1.94 eV	
ΔE_{B} (Hydrogen)	0.76, 0.77 eV ^a			

^aFrom reference [7].

and shows a strong tendency to form a near sp^3 hybridisation. The three C(F)–C(NN) σ -bonds of graphene resist stretching; consequently, these atoms are also slightly dragged out of the plane to reduce the stress over bonds. This results in a reduction of the internal angles $\angle C(NN), C(F), C(NN)$ in the hexagonal ring around C(F) from 120.0° to about 115.5° .

We have performed π -orbital axis vector (POAV1) analysis as described in references [16] and [17] to evaluate the nature of the orbitals in fluorinated graphene. This method is based on the coordinates of the conjugated central carbon atom C(F) and the three neighbouring carbon atoms C(NN). POAV1 predicts a deviation from sp^2 to $sp^{2.33}$ hybridisations for the three C(F)–C(NN) σ bonds for a single fluorine adatom. POAV2 analysis can be used to predict the nature of the C–F bond by calculating the degree of the p content in the σ orbitals (sp^n) [18]. The three σ -bonds resist further pulling up of the C(F). This results in a larger C–F bond length and causes $\angle F, C(F), C(NN)$ to be 102.4° compared with the 109.5° characteristic of sp^3 bonding. Analysing the σ - and π -orbitals of atoms using the POAV2 method demonstrates

Table 3. LDA- and PBE-optimised geometries of two same-side fluorine adatoms (singlet state) on graphene for different supercell sizes: 3×3 and 6×6 . The graphene monolayer before adsorption lies in the plane $z = 0$; the centre of mass of the unit cell is pinned during relaxation. $z(C(F))$ and $z(C(NN))$ are the z -coordinates of each carbon C(F) bonded to fluorine and its nearest neighbour C(NN), respectively. The bond lengths of C(F)–F and C(F)–C(NN) are shown. Values of ΔU_B and second adsorption energy ($\Delta E_{B2} = E(G + F) + E(F) - E(G + 2F)$) of two hydrogen adatoms on a 3×3 supercell of graphene using the PBE functional obtained in this work, as well as ΔE_{B2} obtained in a previous work [7] using the PBE functional in a 5×5 cell are shown for comparison with the results of two fluorine adatom on graphene. .

	LDA		PBE	
	3×3 cell	6×6 cell	3×3 cell	6×6 cell
$z(C) - z(C(NN))$	0.48 Å	0.50 Å	0.49 Å	0.50 Å
C–F	1.44 Å	1.45 Å	1.53 Å	1.45 Å
C(F)–C(F)	1.54 Å	1.56 Å	1.56 Å	1.57 Å
C(NN)–C(F)	1.49 Å	1.49 Å	1.50 Å	1.50 Å
$\angle C(NN), C(F), C(F)$	115.81°	115.80°	115.62°	115.64°
$\angle F, C(F), C(F)$	105.59°	105.55°	105.89°	105.84°
$\angle F, C(F), C(NN)$	101.27°	101.62°	101.58°	101.80°
ΔU_B	0.72 eV	0.71 eV	0.68 eV	0.65 eV
ΔU_B (Hydrogen)			1.16 eV	
ΔE_{B2} (Hydrogen)			1.92, 1.93 eV ^a	

^aFrom reference [7].

the formation of $sp^{4.66}$ rehybridisation in the C(F)–F bond, which indicates the great contribution of nearby p_z -orbitals to this bond. Forming $sp^{4.66}$ hybridisation, rather than sp^3 , arises due to the large electro-negativity of fluorine together with the tendency of the σ -bonds to maintain sp^2 hybridisation in the graphene sheet.

In our study of the most stable geometry for two fluorine adatoms on the same side of a graphene sheet, many possible configurations have been investigated. From our calculations of the binding energy ΔE_B , which will be presented in section 3.2, we have found that the most stable geometry is the structure with two fluorine adatoms above two neighbouring carbon atoms. This is about 0.87 eV more stable than the structure with two fluorine adatoms above next-nearest neighbouring carbon atoms. If we denote the two sublattices of graphene’s bipartite hexagonal lattice as A and B, this would mean the most stable bonding occurs when the two adatoms are bonded to two sites of opposite sublattice A and B. A similar conclusion was reached in a PBE study of the adsorption of a second hydrogen adatom on graphene [7].

A fluorine atom has an unpaired electron, which carries a spin moment of $1 \mu_B$ magnetisation, where μ_B is the Bohr magneton. For a fluorine dimer on graphene, two different states with singlet and triplet spin arrangements are possible. In the triplet case, the two parallel spins further avoid each other in accordance with the Pauli exclusion principle, leading to a larger distance between the two fluorine adatoms and causing a larger stretching of the C(F)–F bond (1.47 against 1.44 Å), and consequently decreasing the stability of the structure by 1.5 eV. The C(NN)–C(F) bond length of the singlet state was calculated to be 1.49 Å, which is larger than the corresponding value of 1.47 Å for a single fluorine adatom. C.f., the C–C bond length in graphene is about 1.42 Å. In the case of two fluorine adatoms, each fluorine atom repels the other, pulling the C(F) atoms further out of the plane by about 0.45 Å. This is a sign of more stress on the three C–C(F) σ bonds compared with the single-adatom case.

3.2. Binding energies: single and two adatoms

The binding energy ΔE_B and formation energy ΔE_F of a single adatom or of multiple adatoms on a graphene sheet are difficult to measure directly due to the small size of the defects. Instead, DFT is an ideal tool to provide quantitative estimates of ΔE_B and ΔE_F at low concentrations. ΔE_B is defined as the energy required to separate a single, isolated adatom from the graphene surface to infinity:

$$\Delta E_B = E(G) + E(F) - E(G + F), \quad (1)$$

where $E(F)$ is the total energy of an isolated fluorine atom. $E(G)$ and $E(G + F)$ are the total energies of a large graphene sheet and a singly fluorinated graphene sheet, respectively. ΔE_B is computed to investigate the stability and the strength of the C–F covalent bond of a single fluorine adatom on graphene. We also introduce ΔU_B as the energy required to separate two fluorine adatoms to infinite distance from each other on a graphene sheet. The formation energy ΔE_F per adatom of fluorinated graphene relative to pristine graphene and the F_2 free molecule is another quantity that characterises the

stability of single-side fluorinated graphene [3, 19, 20]. From these definitions, ΔU_B and ΔE_F can be calculated by:

$$\begin{aligned}\Delta U_B &= E(G) + 2E(F) - 2\Delta E_B - E(G + 2F) \\ &= 2E(G + F) - E(G) - E(G + 2F).\end{aligned}\quad (2)$$

and

$$\Delta E_F = [E(G) + E(F_2) - E(G + 2F)]/2, \quad (3)$$

where ΔE_B is given by equation (1). $E(G + 2F)$ is the total energies of a graphene sheet with a pair of fluorine adatoms placed in stable positions roughly above two neighbouring carbon sites (see figure 2(b)) and $E(F_2)$ is the total energy of a free F_2 molecule. Special care was taken to ensure that the same \mathbf{k} points were used in the graphene and fluorinated graphene calculations. For example, one must use a $15 \times 15 \times 1$ \mathbf{k} -point grid centred on Γ for a primitive cell of graphene to compare its energy $E(G)$ (scaled up to the supercell size) with the energy of fluorinated graphene $E(G + F)$ in a 3×3 supercell with a $5 \times 5 \times 1$ \mathbf{k} -point grid centred on Γ .

From the definitions given in equations (1)–(3), a *negative* value for ΔE_B , ΔU_B or ΔE_F would indicate that the fluorine dimer on graphene is unbound. The predicted values of ΔE_B and ΔU_B at various cell sizes are shown in tables 1, 2 and 3. The PBE values of ΔE_B , ΔE_F and ΔU_B obtained in a 6×6 supercell are 1.95, 1.07 and 0.65 eV, respectively, while the corresponding LDA values are 2.36, 1.20 and 0.71 eV.

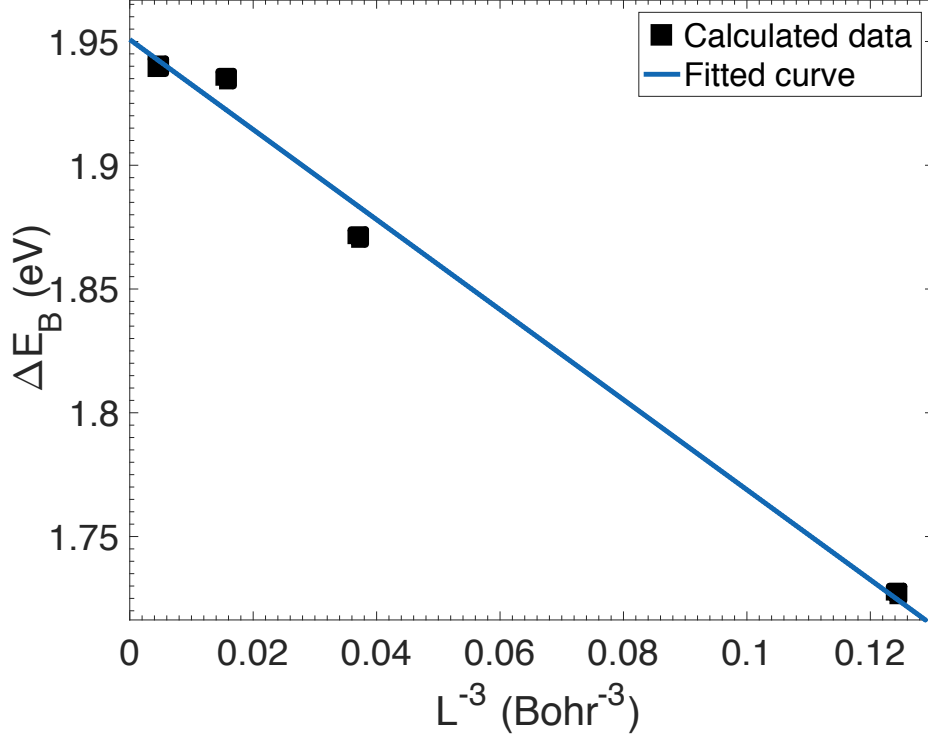
The binding energies ΔE_B of single fluorine adatoms on 3×3 and 4×4 supercells of graphene were calculated in reference [21] using the Perdew–Wang (PW) generalised gradient approximation (GGA) exchange–correlation functional [22] using the projector-augmented-wave (PAW) method, but the value obtained in the dilute limit is about 0.41 eV higher than our PBE results. We believe the difference between our results and those of reference [21] is due to the small plane-wave cutoff (18.37 a.u.) applied in that work. We found that a plane-wave cutoff energy of 28 a.u. is required for adequate convergence within the PAW method. We verified that the GGA-PBE functional over-binds by a similar amount (binding energy of 2.23 eV) when a cutoff energy of 18.37 a.u. is used.

Finite-size effects are a systematic source of errors in our calculations. Finite-size errors arise from the non-physical and unwanted interactions between the periodic images of the adatoms within the plane of the graphene sheet. Löwdin population analysis [23] shows that a relatively large charge of about $0.38|e|$ is transferred from C(F) to the fluorine adatom, giving ionic character to the C(F)–F covalent bond and causing the defect to have a nonzero electric dipole moment. The unwanted electrostatic energy of a 2D lattice of identical dipole moments is positive and falls off as L^{-3} , where L is the linear size of the cell [24]. The function

$$\Delta E_B(L) = \Delta E_B(\infty) + cL^{-3}, \quad (4)$$

was fitted to our PBE results, where $\Delta E_B(L)$ is the ΔE_B value in a cell of linear size L . The extrapolation is shown in figure 2. Note that the positive error in $E(G + F)$ results in c being negative. The binding energy $\Delta E_B(\infty)$ in the dilute limit is 1.95 eV.

Figure 2. PBE binding energy of a single fluorine adatom on an $m \times m$ ($m = 2, 3, 4$ and 6) periodic supercell of graphene (black squares). The binding energy is extrapolated to the dilute limit of infinite cell size ($L \rightarrow \infty$) by fitting equation (4) to the data. The fitted parameter values are $\Delta E_B(\infty) = 1.95$ eV and $c = -1.82$ eV a_0^3 , with the root-mean-square error being 0.02 eV.



As can be seen in figure 2, there are also non-systematic finite-size effects in the binding energy due to the choice of \mathbf{k} -point sampling, long-range oscillations in the charge density around the defect and the strain field resulting from the geometric distortion of the graphene lattice due to the fluorine defect. In general, as the supercell size is increased, the Brillouin zone to be sampled shrinks and hence the required number of \mathbf{k} points decreases in inverse proportion to the supercell size. The results in tables 4 and 5 indicate that the binding energy ΔE_B converges to better than 10 meV with a $7 \times 7 \times 1$ Monkhorst–Pack \mathbf{k} -point mesh in a 3×3 fluorinated graphene supercell, while for a larger 4×4 supercell it is converged to this level with a $5 \times 5 \times 1$ \mathbf{k} -point grid. The bond lengths and angles at each supercell size are listed in tables 1, 2 and 3. These show that the atomic structure in the vicinity of the defect has converged to a high degree of precision in a 6×6 supercell, suggesting that finite-size errors in the binding energy due to geometrical effects may be small.

As described in section 3.1, and in agreement with a previous study [7], we found that two fluorine adatoms on top of two nearest-neighbour carbon atoms belonging to the hexagonal A and B sublattices, respectively, is the most stable single-side two-fluorine-adatom arrangement. The spin part of the ground state can be either a spin-paired singlet ($\uparrow\downarrow$) or a spin-unpaired triplet ($\uparrow\uparrow$) state. In the spin-unpaired arrangement,

the two parallel spins further avoid each other, which leads to an increase in the total energy such that both LDA and PBE calculations predict ΔU_B to take a negative value, as can be seen in table 2. Consequently, two parallel-spin fluorine adatoms are expected to repel each other, and clustering can only be made from anti-parallel spins from adatoms on nearest neighbours. In accordance with the LDA's general tendency to over-bind compared to the PBE functional [25], the absolute value of ΔE_B predicted by the LDA differs by about 0.41 eV from the value predicted by the PBE functional. The over-binding of singly fluorinated graphene predicted by the LDA is associated with the smaller C(F)–F bond length predicted by this functional. PBE and LDA converge to the same C(F)–F bond length of 1.45 Å for a fluorine dimer on graphene; correspondingly the predicted ΔU_B from LDA and PBE calculations are almost the same (the LDA ΔU_B value is only 0.02 eV lower than the PBE value).

The electronic behaviour of fluorine adatoms on graphene differs from that of hydrogen adatoms. For the second *hydrogen* added to graphene, we find that $\Delta U_B =$

Table 4. Relative total energies $\Delta E(G + F)$ and binding energies of a single fluorine adatom on a $m \times m$ supercell of graphene. Data are obtained using different Monkhorst–Pack \mathbf{k} -point grids in the Brillouin zone and supercells with different size. Here, $\Delta E(G + F) = E(G + F)_{k \times k \times 1} - E(G + F)_{l \times l \times 1}$, in which the numbers k and l represent the \mathbf{k} -point grid used in the row numbers $n + 1$ and n ($n = 1 \dots 5$) of this table, respectively.

\mathbf{k} -point mesh	$\Delta E(G + F)$ (meV)		ΔE_B (eV)	
	3×3 cell	4×4 cell	3×3 cell	4×4 cell
$3 \times 3 \times 1$	0.00	0.00	2.04	2.04
$5 \times 5 \times 1$	21.28	−2.72	1.94	1.93
$7 \times 7 \times 1$	−17.42	−5.44	1.90	1.94
$9 \times 9 \times 1$	3.86	5.44	1.90	1.95
$11 \times 11 \times 1$	3.62	0.00	1.90	1.94

Table 5. Relative total energies $\Delta E(G + F)$ and binding energies of a single fluorine adatom on a supercell of graphene. Data are obtained from different Monkhorst–Pack grids in the Brillouin zone of a 6×6 supercell. Here, $\Delta E(G + F) = E(G + F)_{k \times k \times 1} - E(G + F)_{l \times l \times 1}$, in which the numbers k and l represent the \mathbf{k} -point grid used in the row numbers $n + 1$ and n ($n = 1, 2, 3$) of this table, respectively.

\mathbf{k} -point mesh	$\Delta E(G + F)$ (meV)	ΔE_B (eV)
$3 \times 3 \times 1$	0.00	2.03
$5 \times 5 \times 1$	8.16	1.97
$7 \times 7 \times 1$	2.72	1.96

1.16 eV, which is even larger than the first adsorption energy ($\Delta E_B = 0.76$ eV), as seen in table 2, and from the first and second adsorption energies presented in a previous study [7]. In fact, the second adatom couples to the unpaired electron available on the nearest-neighbour site. Fluorine is a strongly electro-negative element and has a great tendency to bind to carbon. Unlike hydrogen, however, there is a significant repulsive interaction between pairs of fluorine adatoms on neighbouring sites due to the overlap between their relatively delocalised orbitals, which decreases ΔU_B . Nevertheless, the experimental F–F bond energy (1.61 eV) is significantly smaller than the C–F bond energy (5.03 eV); in contrast, the H–H bond energy (4.48 eV) is larger than that of C–H (4.26 eV) [26]. Hence fluorinated graphene is more stable than hydrogenated graphene, despite the repulsive interaction between the fluorine atoms on neighbouring carbon atoms.

The LDA and PBE formation energies of a single fluorine adatom on a 3×3 supercell of graphene are about $\Delta E_F = 1.17$ and 0.99 eV, respectively. These values hardly change as the cell size is increased. The *positive* formation energy and ΔU_B indicate that single-side fluorinated graphene is stable, while these values are about two orders of magnitude higher than typical room temperature (~ 26 meV). This thermal stability makes fluorinated graphene distinctive from hydrogenated graphene and potentially more suitable for electronic and spintronic applications. Interestingly, while the binding energies of hydrogenated and fluorinated graphene are not so different, there is a significant difference in their formation energy. The formation energy is a measure of stability against molecular desorption from the graphene surface. In contrast to fluorinated graphene, hydrogenated graphene readily dissociates into graphene and H_2 molecules [3]. The different behaviour is the result of the large difference in the F–F and H–H bond energies, as explained in section 3.2.

3.3. Binding energies: three adatoms

In section 3.2 we found that, for a second fluorine adatom on graphene, it is energetically favourable to keep the two sublattices in balance, with the least possible magnetisation. To understand further the fluorination process, we have studied the behaviour of three fluorine adatoms on 3×3 and 5×5 supercells of graphene. We have applied the general definition of the binding energy per adatom:

$$\overline{\Delta E_B} = \frac{E(G) + n_F E(F) - E(G + n_F F)}{n_F}, \quad (5)$$

where n_F is the number of fluorine adatoms. We have investigated the different possible configurations of the three adatoms on top of the carbon atoms in a hexagonal ring, as shown in figure 3. We refer to the different arrangements of fluorine atoms shown in figure 3 as AAA, ABA, AAA' and AAB'. We find that binding the three fluorine atoms to three carbons from the same sublattice in the AAA arrangement is the least favorable configuration ($\overline{\Delta E_B} = 1.69$ and 1.60 eV per fluorine adatom in a 3×3 and 5×5 cell, respectively). With the exception of the AAA arrangement, the z -coordinates

of the three C(F) atoms differ by about 0.1 Å. In the ABA structure, the z -coordinate of C(F) is larger at the B site; in the AAB' and AAA' structures the z -coordinate of the isolated C(F) atom is smaller than that of the other two C(F) atoms.

Binding-energy results are listed in tables 6 and 7. As in the adsorption of two adatoms, it is energetically favourable to reduce the imbalance between the two sublattices by adsorption on mixed sites. Correspondingly, ABA is the most favoured arrangement by about 1 eV in both supercells. The C–F bond length also is the least for the ABA arrangement. After adsorption of two adatoms on different sites of the A and B sublattices, there is no significant preference in the bonding of a third adatom to a carbon placed in the A or B sublattice. For example, the difference between $\overline{\Delta E_B}$ in ABA ($\overline{\Delta E_B} = 2.10$ eV per fluorine adatom) and ABB ($\overline{\Delta E_B} = 2.09$ eV per fluorine adatom) arrangements in the 3×3 supercell is small. The larger 5×5 cell allows us to inspect the change in binding energy when the third adatom is far from the first ad-dimer. We found that the third fluorine in a mixed-site arrangement, such as AAB', is favored over the same sites arrangements AAA or AAA'; see tables 7 and 3. Moreover, we compared the energy required to separate three adatoms from AAB and AAA configuration to infinite distance from each other using the general equation:

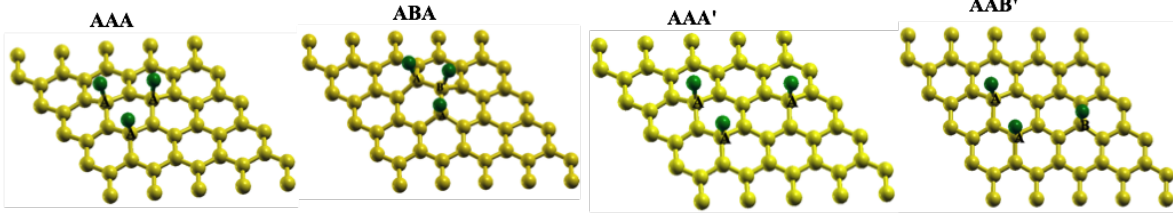
$$\overline{\Delta U_B} = E(G) + n_F E(F) - n_F \overline{\Delta E_B} - E(G + n_F F), \quad (6)$$

where n_F is the number of fluorine adatoms. The results are listed in table 7. We observe that, in contrast to ABA, the AAA arrangement has a negative $\overline{\Delta U_B}$ value and is therefore not a stable arrangement. These outcomes, along with the previous results obtained for an ad-dimer in the section 3.2, suggest that fluorination develops geometrically from a central carbon, with additional fluorine adatoms bonding to neighbouring carbon atoms, and so on.

Another interesting result is that the value of the total magnetisation decreases with increasing binding energy $\overline{\Delta E_B}$, as predicted by the PBE functional. In general, semi-local functionals such as PBE cannot reliably predict the total magnetisation of a fluorine adatom on graphene [27], and more sophisticated methods are needed for quantitative results. The non-integer total magnetisations presented in tables 6 and 7 are due to the need for a more advanced level of theory than DFT-GGA. However, at least we can use the prediction of the PBE functional to compare qualitatively the trend of the change in the total magnetisation in terms of the binding energies. According to PBE, the total magnetisation M is the least for the most stable arrangements listed in tables 6 and 7.

The total energies of three fluorine adatoms on graphene obtained in spin-polarised calculations are typically lower than the energies obtained in spin-unpolarised calculations by about 184 meV in a 3×3 cell. To get more insight into the effects of spin configuration on the binding energy, we have also performed magnetisation-constrained calculations for ABA, which is the most stable configuration in a 3×3 cell. Our results again show that the configuration with two paired spins ($\uparrow\downarrow\uparrow$) is preferred over three parallel spin ($\uparrow\uparrow\uparrow$) by about 748 meV per adatom. This is consistent with

Figure 3. Different arrangements of three fluorine adatoms on graphene. The bonding site is labelled as A or B, depending on the associated sublattice. The prime denotes an arrangement with a third adatom on a non-neighbouring carbon atom.



Lieb's theorem [28], and explains the experimental observation in which the measured number of paramagnetic centres is three orders of magnitude less than the number of fluorine adatoms in fluorinated graphene samples [9]. Also, according to Lieb's theorem, the ground state of a bipartite lattice with a half-filled band has a total spin of $|n_A - n_B|/2$. For pristine graphene the numbers of sites in the A and B sublattices are equal ($n_A = n_B$), leaving the ground state of pristine graphene with zero net spin. For

Table 6. Relative total energy of adatoms on graphene in a 3×3 supercell (compared to the total energy of the AAA configuration of adatoms), binding energies per adatom, PBE magnetic moment in units of μ_B , $|n_A - n_B|/2$, and the energy of the unpaired-spin configuration relative to the paired-spin configuration: $\Delta E_S = E(\uparrow\uparrow\uparrow) - E(\uparrow\downarrow\uparrow)$. n_A and n_B are the numbers of fluorine adatoms above carbon atoms on the A and B hexagonal sublattices, respectively.

Configuration	$\Delta E(G + 3F)$ (eV)	$\overline{\Delta E_B}$ (eV)	M (μ_B)	$ n_A - n_B /2$	ΔE_S (eV)
ABA	-1.25	2.10	0.28	1/2	0.75
BAB	-1.22	2.09	0.43	1/2	
AAA	0.00	1.69	1	3/2	

Table 7. Relative total energy of three fluorine adatoms on graphene in a 5×5 supercell (compared to the total energy of the AAA configuration of adatoms), binding energy per adatom, energy required to separate three fluorine adatoms to infinite distance, PBE predicted magnetic moment in units of μ_B and $|n_A - n_B|/2$. The C(F)-F bond length of each arrangement shown in figure 3 is also listed.

Config.	$\Delta E(G + 3F)$ (eV)	$\overline{\Delta E_B}$ (eV)	$\overline{\Delta U_B}$ (eV)	M (μ_B)	$ n_A - n_B /2$	C-F (\AA)
AAA	0.00	1.60	-0.34	1	3/2	1.52
ABA	-0.98	1.94	0.64	0	1/2	1.46
AAA'	0.02	1.60	-0.36	0.5	3/2	1.55
AAB'	-0.35	1.73	0.01	0	1/2	1.53

the ABA arrangement of fluorine adatoms on graphene, for which $n_A = N/2 - 2$ and $n_B = N/2 - 1$, S should be equal to $1/2$, which leaves an unpaired spin (for example $\uparrow\downarrow\uparrow$ configuration against $\uparrow\uparrow\uparrow$ spin-arrangement) with total magnetisation $M = 1 \mu_B$. The same outcomes are deduced when two and three hydrogen atoms are adsorbed on the graphene sheet [7]. All these results lead us to conclude that when two or more fluorine atoms with unpaired spins are adsorbed on graphene, long-ranged spin polarisations, of opposite signs are induced in the two sublattices to reduce the total magnetisation. So we see that ABA and ABA' with the least magnetisations are energetically similar (ABA is preferred), and are the most stable configurations. This interpretation from the energies point of view has been deduced explicitly by higher-level calculations using a hybrid functional or a DFT+U model [27, 29].

4. Conclusions

In summary, we have studied the orbital nature of the C-F bond in fluorinated graphene. Using the POAV method we find $sp^{4.6}$ rehybridisation for the C-F bond of a single fluorine adatom on a graphene sheet, implying large contributions from nearby p orbitals. The behaviour of the binding energy of a fluorine adatom on graphene in supercells of various sizes was investigated, and the results were compared with hydrogenated graphene within the DFT framework. Both the LDA and PBE functionals predict that a fluorine dimer adsorbed onto neighbouring carbon atoms is a stable structure, suggesting that there should be a tendency for fluorine atoms to cluster during a fluorination process in which a single side of graphene is exposed to fluorine. Our calculations show that, in contrast to hydrogenated graphene, the formation energy of single-side fluorinated graphene is positive, which implies fluorinated graphene should be more stable than hydrogenated graphene at higher temperature. Also, for multiple fluorine adatoms the configurations in which the fluorine atoms are bonded to sites corresponding to the same sublattice are less stable. This suggests that fluorination proceeds with fluorine atoms successively bonding to neighbouring carbon atoms. The spins density of states in the ground state are arranged according to minimise the total magnetisation. We have shown that the finite-size error in the binding energy of isolated fluorine adatoms or ad-dimers stems from the interaction of the electric dipole moments of images of the defects in neighbouring cells, and falls off as the inverse cube of the linear cell size.

5. Acknowledgements

F Marsusi appreciates the computer assistance provided by Mrs Z Zeinali in the Department of Energy Engineering and Physics at Amirkabir University of Technology.

- [1] Han W, Kawakami R K, Gmitra M and Fabian J 2014 *Nat. Nanotechnol.* **9** 794
- [2] Boukhvalov D W 2010 *Physica E* **43** 199
- [3] Yi D, Yang L, Xie S and Saxena A 2015 *RSC Adv.* **5** 20617
- [4] Feng W, Long P, Feng Y and Li Y 2016 *Adv. Sci.* **3** 1500413
- [5] Nair R R, Ren W, Jalil R, Riaz I, Kravets V G, Britnell L, Blake P, Schedin F, Mayorov A S, Yuan S, Katsnelson M I, Cheng H-M, Strupinski W, Bulusheva L G, Okotrub A V, Grigorieva I V, Grigorenko A N, Novoselov K S and Geim A K 2010 *Small* **6** 2877
- [6] Şahin H H, Topsakal M and Ciraci S 2011 *Phys. Rev. B* **83** 115432
- [7] Casolo S, Løvvik O M, Martinazzo R and Tantardini G F 2009 *J. Chem. Phys.* **130** 054704
- [8] Nakada K and Ishii A 2011 “Graphene Simulation” 1st ed. InTech Open Access Publisher Chap. 1
- [9] Nair R R, Sepioni M, Tsai I L, Lehtinen O, Keinonen J, Krashennnikov A V, Thomson T, Geim A K and Grigorieva I V 2012 *Nat. Physics* **8** 199
- [10] Gonze X, Amadon B, Anglade P-M, Beuken J-M, Bottin F, Boulanger P, Bruneval F, Caliste D, Caracas R, Côté M *et al.* 2009 *Computer Phys. Comm.* **180** 2582
- [11] Perdew J P, Burke K and Ernzerhof M 1996 *Phys. Rev. Lett.* **77** 3865
- [12] Monkhorst J and Pack J D 1976 *Phys. Rev. B* **13** 5188
- [13] Troullier N and Martins J L 1991 *Phys. Rev. B* **43** 1993
- [14] http://www.abinit.org/downloads/psp-links/lda_tm
- [15] Santos E J G, Ayuela A and Sánchez-Portal D 2012 *New J. Phys.* **14**, 043022
- [16] Haddon R C 1986 *Chem. Phys. Lett.* **125** 231
- [17] Bai H, Zhu Y, Yuan N, Ji Y, Qiao W and Huang Y 2013 *Chinese J. Struct. Chem.* **32** 695
- [18] Haddon R C and Scott L T 1986 *Pure Appl. Chem.* **58** 137
- [19] Sofo J O, Chaudhari A S and Barber G D 2007 *Phys. Rev. B* **75** 153401
- [20] Leenaerts O, Peelaers H, Hernández-Nieves A D, Partoens B and Peeters F M 2010 *Phys. Rev. B* **82** 195436
- [21] Liu H Y, Hou Z F, Hu C H, Yang Y and Zhu Z Z 2012 *J. Phys. Chem. C* **116** 18193
- [22] Perdew J P and Wang Y 1992 *Phys. Rev. B* **45** 13244
- [23] Löwdin P O 1955 *Phys. Rev.* **97** 1474
- [24] Makov G and Payne M C 1995 *Phys. Rev. B* **51** 4014
- [25] Groß A 2003 *Theoretical Surface Science: A Microscopic Perspective*, Chap. 3, Springer, New York
- [26] “National Standard Reference Data Series”, National Bureau of Standards, No. **31**, Washington, DC, 1970; Benson S W 1965 *J. Chem. Educ.* **42** 502
- [27] Kim H J and Cho J H 2013 *Phys. Rev. B* **87** 174435
- [28] Lieb E H 1989 *Phys. Rev. Lett.* **62** 1201
- [29] Marsusi F and Verstraete M J to be published